Article citation info:
Jasion P, Magnucki K. Bending of the three-span rail (UIC 60) subjected to the concentrated force. Rail Vehicles/Pojazdy Szynowe. 2025;1-2:32-38. https://doi.org/10.53502/RAIL-211433

Rail Vehicles/Pojazdy Szynowe

www.railvehicles.eu

Bending of the three-span rail (UIC 60) subjected to the concentrated force

Paweł **Jasion** [a, *], Krzytof **Magnucki** [b]

[a] *Faculty of Mechanical Engineering, Poznan University of Technology, Poznan, Poland*
[b] *Łukasiewicz Research Network – Poznan Institute of Technology, Poznan, Poland*

ARTICLE INFO

Received: 20 August 2025
Revised: 10 September 2025
Accepted: 27 September 2025
Available online: 13 October 2025

KEYWORDS

Rail UIC 60
Timoshenko beam theory
Bending
Analytical studies
Numerical FEM studies

The subject of the paper is the three-span rail (UIC 60) simply supported on four sleepers. The middle span is subject to the concentrated force at half of its length. The goal of the investigation is to analyse the influence of the shear stresses on the bending of the reail. For this reason analytical study of the bending problem of the three parts of this rail is realized with consideration of the Timoshenko beam theory. Moreover, the problem is studied numerically using the finite element method (FEM). Based on the obtained analytical results it is seen that structures like rails, which between the speepers can be treated as short beams, should be analysed with shear effect taking into account. The result obtained this way is consistent with the results of numerical investigation. Ignoring the shear effect results in a significant underestimation of the deflection. The obtained analytical solution may serve as a simple tool for designing I-beam-like structures having in mind the shear stresses.

1. Introduction

Modern railways require tracks capable of carrying the loads of high-speed trains and at the same time compliant with safety regulations. To meet these requirements proper design and structural analyses are necessary to describe the behaviour of rail tracks under the load of trains. The problems that may arise during design can be analysed in the laboratory and this approach is widely used. However, nowadays the analysis of many phenomena is possible using numerical tools. One of them is the finite element method (FEM) which is also used in railway tracks related problems. An example is the work by Al Gharavi et al. [5] in which a three-point bending test is made for bolted and welded connection in the UIC 60 rail both, using experiment and FE analysis. He et al. [6] used FEM to analyse the wear phenomenon and contact stress which appear at the junction of the wheel and the rail.

Another typical problem is the failure analysis which can be related either to the rail, the head of which is prone to fatigue cracking as shown by Afridi et al. [1] in FEM/BEM simulations or to the concrete sleeper in which corrosion as well as cracks may appear during exploitation as presented by Camille et al. [3] in experimental tests. A well-known problem in rail transportation is the rolling noise. It is related to the vibrations of the rail which can be analysed with the FEM as shown by Knuth et al. [10]. Authors present the model which gives the possibility to take into account the change of the cross-section's shape resulting from vibrations.

Under the load the rail bends between the sleepers and its deflection, related to the spacing of the sleepers and shape of the cross-section of the rail, influences the behaviour of the whole railway track. To analyse the deflection the rail must be treated like a beam on multiple supports and calculated taking into account the shear stresses. Thus, a proper beam theory must be applied. Timoshenko [14] in 1921 initiated the analytical consideration of the shear effect in beams. Gere and Timoshenko [4] described in detail the problems of tension-compression of bars, torsion of shafts, bending of beams with consideration of a shear effect, theory of thin-walled open sections, an inelastic bending of beams, and buckling problems of columns. Wang et al. [16] presented in the following

* Corresponding author: pawel.jasion@put.poznan.pl (P. Jasion)

chapters the beam theories: Euler-Bernoulli (EBT), Timoshenko (TBT), Reddy-Bickford (RBT). Authors also analysed the relationships between (EBT) and (TBT) theories as well as between (EBT) and (RBT). The applications of these theories in plate analysis were also investigated. Hutchinson [7] presented the Timoshenko beam theory, taking into account a new formula of the shear coefficients for various beam cross sections. Kennedy et al. [9] developed a novel theory of layered orthotropic beams taking into account the Timoshenko beam theory and determined new expressions for the shear correction factor. Roque et al. [13] analysed the bending behaviour of laminated composite beams using a modified couple stress theory and a meshless method taking into account the Timoshenko beam theory.

Romanoff and Reddy [12] carried out experimental validation of the modified Timoshenko beam theory for sandwich panels and experimentally demonstrated the correctness of the developed theory. Wang et al. [15] studied analytically and numerically wave propagation in metal foam beams based on the Euler–Bernoulli and Timoshenko beam theories. The porosity distribution in the depth direction of these beams was symmetrical and asymmetrical. Katili et al. [8] developed the two-node beam element with Hermitian functions (4 degrees of freedom in the node) with consideration of the modified Timoshenko beam theory and studied natural frequencies of rectangular functionally graded material (FGM) beam with different boundary conditions. Nampally and Reddy [11] presented the von Kármán nonlinear strains and the nonlinear Cosserat deformation gradient for the moderate rotations of normal planes into the Euler–Bernoulli and the Timoshenko micropolar beam theories. Moreover, they presented numerical examples illustrating the influence of the number of couplings and the length scale of the bending characteristic on the deflections and microrotations. Ahmed and Rifai [2] highlighted the important problem of understanding the strategy of the method of analysis relating to the physical basics of the problem and mastering mathematical tools. They presented a detailed review of Euler-Bernoulli and Timoshenko beam theories and their applications in analytical and numerical studies of beams and plates.

The subject of the present work is the three-span standard rail (UIC 60) of total length 3L and depth h simply supported on four sleepers (Fig. 1). The middle span is subject to the concentrated force at half of its length.

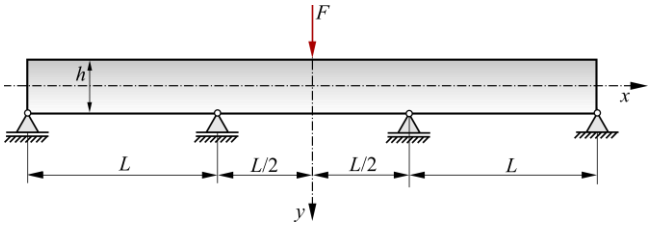

Fig. 1. Scheme of three rail spans with load – force F

The main goal of this paper is analytical and numerical (FEM) studies of the rail deflections under the concentrated force and their comparison.

2. Analytical study of the rail bending

Analytical study of the beam bending is carried out according to Timoshenko beam theory. Thus, taking into account the book [2], the differential equation of the beam deflection line, with consideration of the shear effect, is in the following form

$$\mathrm{EJ_z}\frac{\mathrm{d}^2\mathrm{v}}{\mathrm{dx}^2} = -\mathrm{M_b(x)} + 2(1+\nu)\frac{\mathrm{J_z}}{\mathrm{A}}\alpha_\mathrm{s}\frac{\mathrm{dT}}{\mathrm{dx}} \tag{1}$$

and after integration

$$\mathrm{EJ_z}\frac{\mathrm{dv}}{\mathrm{dx}} = \mathrm{C_1} - \int \mathrm{M_b(x)dx} + 2(1+\nu)\frac{\mathrm{J_z}}{\mathrm{A}}\alpha_\mathrm{s}\mathrm{T(x)} \tag{2}$$

where: $\mathrm{v(x)}$ – deflection, $\mathrm{M_b(x)}$ – bending moment, $\mathrm{T(x)}$ – transverse shear force, α_s – shear coefficient, $\mathrm{J_z}$ – inertia moment of the cross section, A – area of the cross section, E – Young's modulus, ν – Poisson ratio.

The shear coefficient α_s, based on the book [2], is approximately defined for I-beam cross section as follows

$$\alpha_\mathrm{s} = \frac{\mathrm{A}}{\mathrm{A_w}} \tag{3}$$

where the area of the web

$$\mathrm{A_w} = \mathrm{b_w h_w} \tag{4}$$

In the above formula $\mathrm{b_w}$ is the web thickness and $\mathrm{h_w}$ is the web depth. This expression (3) can be conveniently applied to the analytical study of the rail bending.

2.1. Analytical determination of the rail deflection

This three-span rail (Fig. 1) is a symmetrical construction, therefore, the analytical model is developed for its half (Fig. 2).

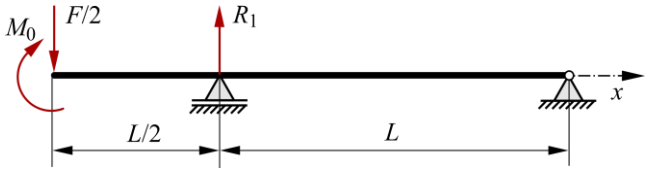

Fig. 2. Scheme of loads acting on the rail

Based on Fig. 2 the equilibrium equation, the bending moment in the middle of the rail, has the form

$$M_o = \frac{3}{4}FL - R_1 L \tag{5}$$

Analytical determination of deflections in successive spans (Fig. 2) will be described in two steps, separately for the middle and the right span. First, for the middle span the coordinate x varies within the range $0 \le x \le \frac{1}{2}L$. The internal forces have the form

$$T_1(x) = -\frac{1}{2}F \tag{6}$$

$$M_{b1}(x) = M_o - \frac{1}{2}F\,x \tag{7}$$

Taking into account equation (2), after simply transformation, it can be written as

$$EJ_z \frac{dv_1}{dx} = -M_o x + \frac{1}{4}Fx^2 - (1+\nu)\frac{J_z}{A_w}F \tag{8}$$

Integrating this equation, one obtains

$$EJ_z v_1(x) = C_2 - \frac{1}{2}M_o x^2 + \frac{1}{12}Fx^3 - (1+\nu)\frac{J_z}{A_w}Fx \tag{9}$$

From the condition $v_1(L/2) = 0$, the integration constant can be determined in the form

$$C_2 = \frac{1}{8}M_o L^2 - \frac{1}{96}FL^3 + (1+\nu)\frac{J_z}{A_w}FL \tag{10}$$

Thus, the deflection line of the middle half of the span in the dimensionless coordinate $\xi = x/L$, is in the following form

$$v_1(\xi) = \Big[12(1-4\xi^2)\bar{M}_o - 1 + 8\xi^3 + 48(1+\nu)\frac{J_z}{A_w L^2}(1-2\xi)\Big]\frac{FL^3}{96EJ_z}, \tag{11}$$

where: $\bar{M}_o = \frac{M_o}{FL}$ – unknown dimensionless moment in the middle of the rail.

Second, for the right span the coordinate x varies within the range $\frac{1}{2}L \le x \le \frac{3}{2}L$, and the internal forces take the following form

$$T_2(x) = \frac{1}{2}(2R_1 - F) \tag{12}$$

$$M_{b2}(x) = M_o - \frac{1}{2}F\,x + R_1\left(x - \frac{1}{2}L\right) \tag{13}$$

Taking into account the equation (2), after simply transformation, it can be written as

$$EJ_z \frac{dv_2}{dx} = C_3 - M_o x + \frac{1}{4}Fx^2 - \frac{1}{2}R_1(x^2 - Lx) + (1+\nu)\frac{J_z}{A_w}(2R_1 - F) \tag{14}$$

From the condition $dv_1/dx|_{L/2} = dv_2/dx|_{L/2}$, the integration constant can be determined in the following form

$$C_3 = -\frac{1}{8}\Big[1 + 16(1+\nu)\frac{J_z}{A_w L^2}\Big]R_1 L^2 \tag{15}$$

Therefore, the equation (15) is in the form

$$EJ_z \frac{dv_2}{dx} = -M_o x + \frac{1}{4}Fx^2 - \frac{1}{8}R_1\left(L^2 - 4Lx + 4x^2\right) - (1+\nu)\frac{J_z}{A_w}F \tag{16}$$

Integrating this equation, one obtains

$$EJ_z v_2(x) = C_4 - \frac{1}{2}M_o x^2 + \frac{1}{12}Fx^3 - \frac{1}{8}R_1\left(L^2 x - 2Lx^2 + \frac{4}{3}x^3\right) - (1+\nu)\frac{J_z}{A_w}Fx \tag{17}$$

Taking into account two conditions $v_2(L/2) = 0$ and $v_2(3L/2) = 0$, after simply transformation, one obtains the integration constant

$$C_4 = \frac{1}{8}M_o L^2 - \frac{1}{96}FL^3 + \frac{1}{48}R_1 L^3 + \frac{1}{2}(1+\nu)\frac{J_z}{A_w}FL \tag{18}$$

and

$$\bar{M}_o = \frac{7}{40} - \frac{6}{5}(1+\nu)\frac{J_z}{A_w L^2} \tag{19}$$

$$\bar{R}_1 = \frac{23}{40} + \frac{6}{5}(1+\nu)\frac{J_z}{A_w L^2} \tag{20}$$

where: $\bar{R}_1 = R_1/F$ – the dimensionless reaction.

Thus, the deflection line of the right span in the dimensionless coordinate $\xi = x/L$, is in the following form

$$v_2(\xi) = \Big[12(1-4\xi^2)\bar{M}_o - 1 + 8\xi^3 + 2(1 - 6\xi + 12\xi^2 - 8\xi^3)\bar{R}_1 + 48(1+\nu)\frac{J_z}{A_w L^2}(1-2\xi)\Big]\frac{FL^3}{96EJ_z} \tag{21}$$

Therefore, the maximum deflection of the rail in accordance with the solution taking into account the shear effect can be determined from the following formula

$$v_{max}^{(An)} = v_1(0) = \Big[12\bar{M}_o - 1 + 48\frac{J_z}{A_w L^2}\Big]\frac{FL^3}{96EJ_z} \tag{22}$$

For comparison, the maximum deflection of the rail without the shear effect is as follows

$$v_{max}^{(wo)} = [12\bar{M}_o - 1]\frac{FL^3}{96EJ_z} \tag{23}$$

where: $\bar{M}_o = 7/40$.

2.2. Results of analytical calculation of the rail deflection

The data of the three-span rail (UIC 60) are as follows:

$A = 7686\ \text{mm}^2$, $J_z = 3055 \cdot 10^4\ \text{mm}^4$

$L = 600$ mm, $h = 172$ mm, $\lambda = L/h \cong 3.5$
$E = 200000$ MPa, $\nu = 0.3$, $b_w = 16.5$ mm
$h_w = h - (13.3 + 37.5/2) = 140$ mm
$A_w = b_w h_w = 2310$ mm^2.

Thus, the maximum deflection value of the rail (22) is as follows $v_{max}^{(An)} = 0.1100$ mm. While the maximum deflection value of this rail without the shear effect (23) is $v_{max}^{(wo)} = 0.04472$ mm.

The form of the rail deflection line is shown in Fig. 3.

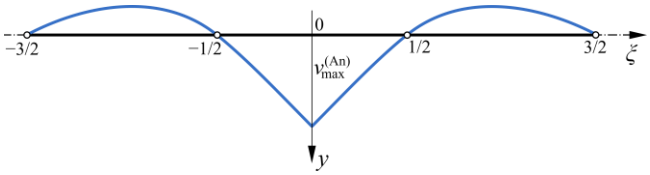

Fig. 3. Scheme of the deflection line of three-span rail

3. Numerical FEM studies of the rail bending

3.1. Numerical FEM model of the rail

Numerical analyses have been performed with the use of Ansys software. The goal was to determine the deflection of the rail thus the linear elastic analysis has been performed with small deflection assumption and linear elastic material model. Assumed parameters for the material were: Young's modulus E = 200,000 MPa and Poisson ratio ν = 0.3.

Due to the symmetry of the problem a half of the UIC 60 rail has been modelled with proper boundary conditions in the mid-length. For comparison reason two variants of boundary conditions have been considered. First one, corresponding to actual structure (Fig. 4a), in which the rail was supported at the bottom and loaded at the upper face. To avoid stress concentration and local indentation due to point boundary conditions the support was realised on the rectangle which spread about 1 mm from the actual edge in both directions. In turn, the load was applied to an ellipse-shaped surface whose dimensions were 10×5 mm.

At the support only vertical displacements were blocked; horizontal displacement was prevented by symmetry conditions. Additionally, to avoid a rigid body motion the displacement along the x axis was prevented at one point in the mid-length of the rail.

The second variant of boundary conditions corresponds to the analytical model which means that they were applied at the neutral axis. For this reason, the remote boundary conditions and remote force options were used available in the system. The conditions were applied to the whole cross-section and brought to the centroid of this section as shown in Fig. 4b.

To discretize the model a second order solid finite element *solid187* has been used with three degrease of freedom in each node. Most of elements were tetrahedrals with 10 nodes. The size of the element has been set to 4 mm which gave in total about 677,000 elements. For improving the application of actual boundary conditions, the size was decreased to 1 mm at the support and at the point of force application. The size of the element was established based on the mesh convergency analysis performed for elements ranging in size from 3 to 8 mm which resulted in meshes consisting of 132,843 and 1,337,870 nodes, respectively. The corresponding maximum deflection v was equal to 0.11975 and 0.11964 mm which suggest that even the biggest size of the element could be used in analyses. However, the selected value of 4 mm provides a smooth distribution of stress and does not require high computational power.

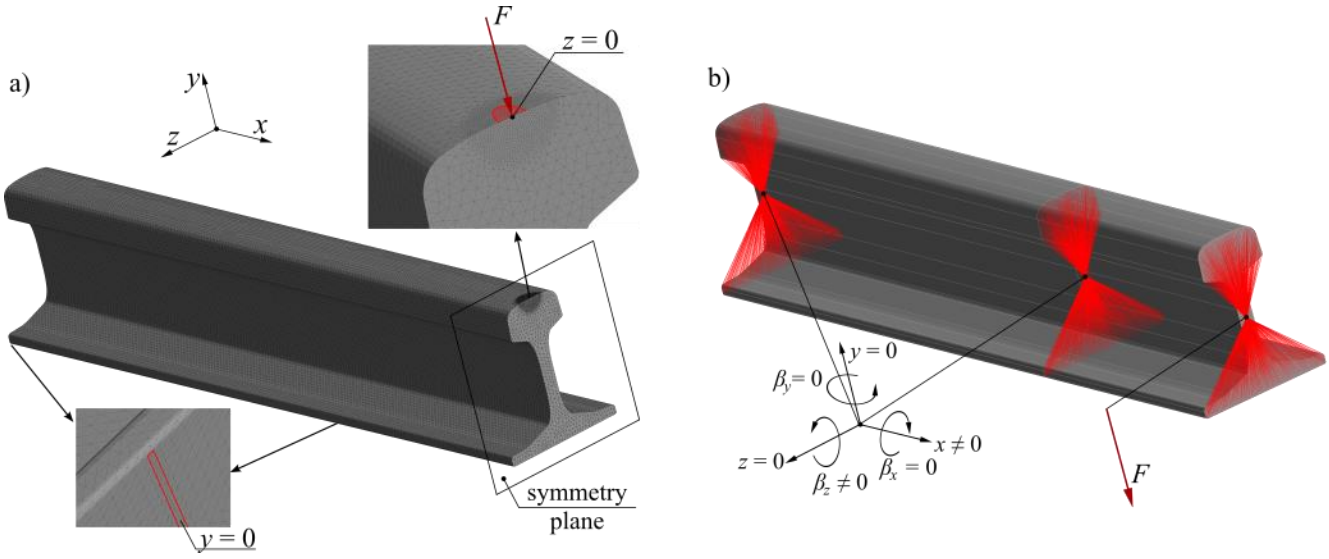

Fig. 4. FE model of the rail: a) actual support conditions; b) support at cross-section

3.2. Results of numerical FEM calculation of the rail deflection

The results of analyses for both FE models are shown in Fig. 5 in the form of plots. Additionally, for the model with actual boundary conditions the vertical displacement of the whole model has been presented in Fig. 5a.

On both plots the horizontal axis corresponds to the length of the rail whereas the vertical one presents the deflection of the rail. Two solutions are shown. The first one, in Fig. 5b, is the deflection of the bottom of the rail, and the second one, in Fig. 5c, the deflection of its neutral line. The plots contain two curves presenting the results for the actual boundary conditions, red curves, and the results for the case of boundary conditions applied to the neutral line, blue curves.

When two curves on both plots are compared it can be seen that the actual boundary conditions results in higher deflection at most points of the rail. The biggest difference occurs in the mid-length of the rail for the deflection of the neutral line. The discrepancy equals 14% – the deflection for the actual boundary conditions equal to 0.1106 mm and for the boundary conditions realised on the neutral line equals 0.12573 mm. However, this is mostly the effect of local indentation which appear at the support due to which the whole rail moves down.

To compare the FE results with the analytical approach presented in section 2, the FE model with boundary conditions realized at the neutral line should be considered. Having this in mind one may see that the results are almost the same. The maximum deflection obtained from the analytical approach, equation (22), is equal to 0.1100 mm whereas the same deflection given by the FE calculations is equal to 0.1106 mm.

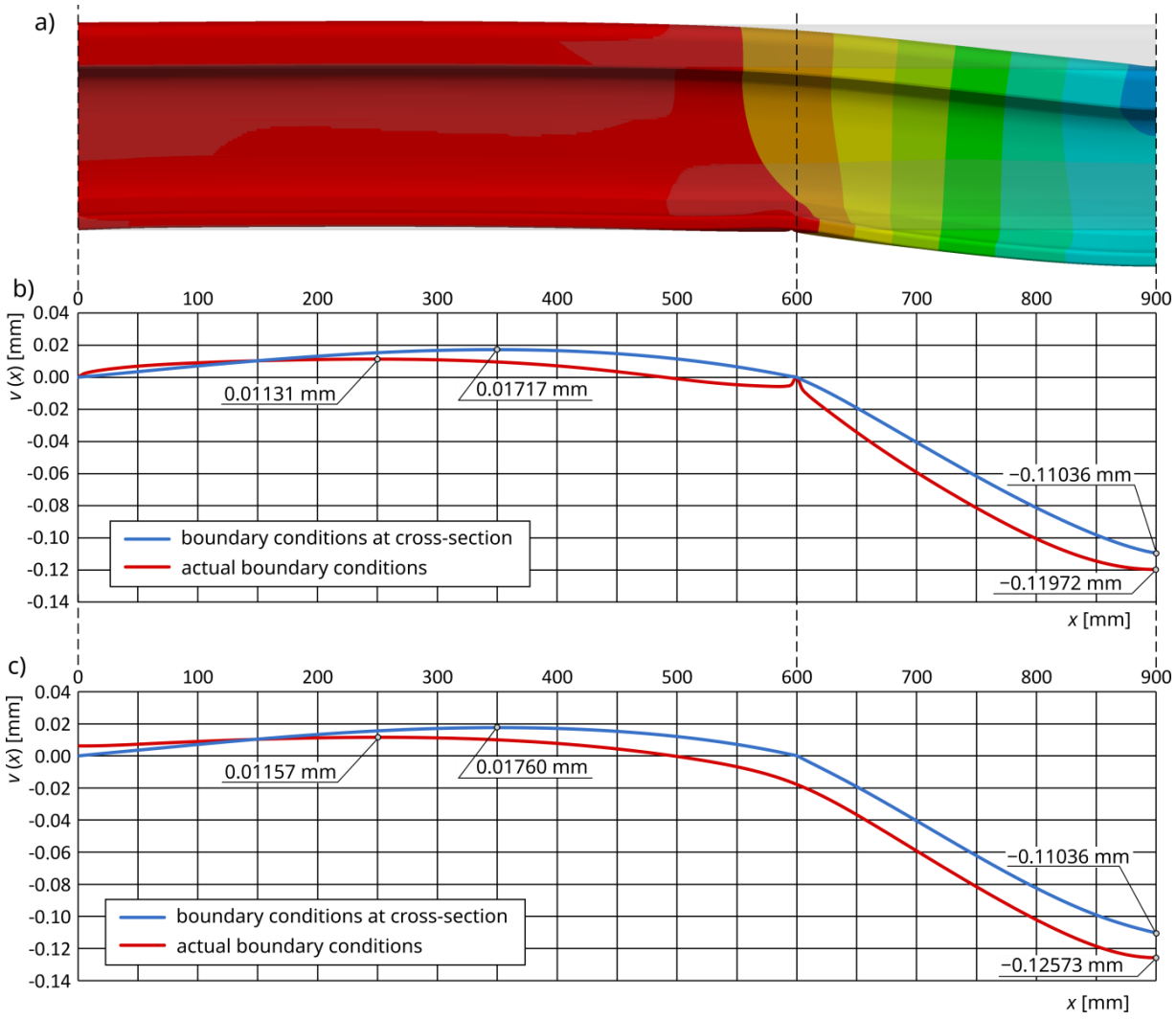

Fig. 5. Deflection of the rail: a) view of the FE result (×200); b) deflection of the bottom; c) deflection of the neutral line

4. Conclusions

In the paper the standard rail UIC 60 has been analysed treated as a beam on four supports. The goal of the investigation was to point out that for such structures shear stresses play a significant role in the deflection analysis. It is easy to see that the relative length of the rail span is very small ($\lambda = L/h \cong 3.5$), therefore, it is necessary to analyze the rail bending taking into account the shear effect. The presented analytical solution with consideration of this effect is consistent with the numerical (FEM) one. On the other hand, the analytical solution without shear effect is significantly smaller, approximately 2.5 times, than the numerical (FEM) one. This shows that taking the shear stresses into account significantly improves the analytical solutions of problems related to short beams and makes them more realistic. The use of classical Euler-Bernoulli theory, valid for relatively long beams, in case of short beams leads to underestimated values. It should be also pointed out, based on the results obtained from FE analysis, that the boundary conditions applied to the presented model influence both the bending behaviour and the value of deflection and should be selected carefully.

The analytical approach presented in the paper allows one to easily determine the deflection of different types of rails or similar structures using equation (22) and determining the shear coefficient from equation (3). Additionally, based on formula (23) one may assess the deflection without shear stresses taken into account. Comparing these two results it is possible to estimate how these stresses influence the behaviour of the analysed structure. All the above-mentioned analytical formulae may simplify the engineering calculations of short I-beam-like structures and may serve as reference point for FE calculations.

Having in mind already obtained results further research can be planned. This may concern analysis of multi-span rails to analyse the behaviour of longer parts of railway tracks also with multiple forces applied which will simulate a train load. Another crucial topic can be the influence of the support stiffness since in actual railway tracks it may vary depending on a number of factors. This stiffness may influence the bending behaviour of the track as well as the behaviour of the train. This in turn may affect the safety of train travel.

Acknowledgements

The paper is developed based on the statutory activity of the Poznan University of Technology (Grant of the Ministry of Science and Higher Education in Poland no 0612/SBAD/3640) and the scientific activity of the Łukasiewicz Research Network – Poznan Institute of Technology.

Bibliography

[1] Afridi AH, Zhu H, Camacho ET, Deng G, Li H. Numerical modeling of rolling contact fatigue cracks in the railhead. Eng Fail Anal Part B. 2023;143: 106838. https://doi.org/10.1016/j.engfailanal.2022.106838

[2] Ahmed AM, Rifai AM. Euler-Bernoulli and Timoshenko beam theories analytical and numerical comprehensive revision. European J Engineer Tech Res. 2021;6(7):20-32. https://doi.org/10.24018/ejers.2021.6.7.2626

[3] Camille C, Mirza O, Kirkland B, Clarke T. Structural behaviour of prestressed concrete sleepers reinforced with high-performance macro synthetic fibres. Eng Fail Anal. 2022;141:106671. https://doi.org/10.1016/j.engfailanal.2022.106671

[4] Gere JM, Timoshenko SP. Mechanics of materials. PWS-KENT Publishing Company: Boston 1984.

[5] Gharawi MA, Saadoon AM, Hmoad NR, Albayati AH. Structural performance of rail connections: experimental testing and finite element modelling. Results Eng. 2025;27:105997. https://doi.org/10.1016/j.rineng.2025.105997

[6] He C, Yang Z, Zhang P, Li S, Naeimi M, Dollevoet R et al. A finite element thermomechanical analysis of the development of wheel polygonal wear. Tribol Int. 2024;195:109577. https://doi.org/10.1016/j.triboint.2024.109577

[7] Hutchinson JR. Shear coefficient for Timoshenko beam theory. ASME J Applied Mech. 2001;68:87-92. https://doi.org/10.1115/1.1349417

[8] Katili I, Syahril T, Katili AM. Static and free vibration analysis of FGM beam based on unified and integrated of Timoshenko's theory. Compos Struct. 2020;242: 112130. https://doi.org/10.1016/j.compstruct.2020.112130

[9] Kennedy GJ, Hansen JS, Martins JRRA. A Timoshenko beam theory with pressure corrections for layered orthotropic beams. 2011;48:2373-2382. https://doi.org/10.1016/j.apm.2013.02.047

[10] Knuth C, Squicciarini G, Thompson D. An efficient model for predicting the sound radiation from a railway rail accounting for cross-section deformation. J Sound Vib. 2025;618, Part B:119323. https://doi.org/10.1016/j.jsv.2025.119323

[11] Nampally P, Reddy JN. Geometrically nonlinear Euler–Bernoulli and Timoshenko micropolar beam theories. Acta Mechanica. 2020;**231**:4217-4242. https://doi.org/10.1007/s00707-020-02764-x

[12] Romanoff J, Reddy JN. Experimental validation of the modified couple stress Timoshenko beam theory for web-core sandwich panels. Compos Struct. 2014;111: 130-137. https://doi.org/10.1016/j.compstruct.2013.11.029

[13] Roque CMC, Fidalgo DS, Ferreira AJM, Reddy JN. A study of a microstructure-dependent composite laminated Timoshenko beam using a modified couple stress theory and a meshless method. Compos Struct. 2013;96:532-537. https://doi.org/10.1016/j.compstruct.2012.09.011

[14] Timoshenko SP. On the correction for shear of the differential equation for transverse vibrations of prismatic bars. Philosophical Magazine. 1921;41:744-746.

[15] Wang YQ, Liang C, Zu JW. Examining wave propagation characteristics in metal foam beams: Euler–Bernoulli and Timoshenko models. J Brazilian Society Mech Sciences Engineering 2018;40:565. https://doi.org/10.1007/s40430-018-1491-z

[16] Wang CM, Reddy JN, Lee KH. Shear deformable beams and plates. Relationships with classical solutions. Amsterdam, Lausanne, New York, Oxford, Shannon, Singapore, Tokyo 2000.